

## ABSTRACT

Structural Modifications of OXi8006 Leading to New Indole-Based Anti-Cancer Agents

Priscilla S. Hor

Director: Kevin G. Pinney, Ph.D.

A promising method for treating cancer involves selectively targeting the tumor vascular network. Tumor vascular is characterized as a disorganized and convoluted network of microvessels, in contrast to normal tissue vasculature, presenting an ideal target for small molecule intervention. Small-molecule anti-cancer agents, known as vascular disrupting agents (VDAs), function by damaging existing tumor vasculature through an essential binding interaction at the dynamic tubulin-protein system effecting vessel occlusion and collapse. This selective binding ultimately deprives tumors of vital nutrients and oxygen necessary for growth resulting in hypoxia and tumor necrosis. A particular benchmark VDA isolated from the bark of the South African bush willow tree *Combretum caffrum* is combretastatin A-4 (CA4). This compound demonstrates exceptional inhibition of tubulin assembly. Previous investigations in the Pinney Lab led to the development of an indole-based VDA modeled after CA4 known as OXi8006. OXi8006 exhibits inhibition of tubulin polymerization comparable to CA4 and demonstrates strong cytotoxicity against human cancer cell lines. In an effort to better understand the biochemical mechanisms of action and fully evaluate the biological activity of OXi8006 sufficient amounts of the compound are necessary. In addition to the resynthesis of OXi8006, structural modifications on the indole scaffold will provide insight into the biological activity and tubulin assembly inhibition with respect to

regioselective functionalizations. In addition, modified analogues of OXi8006 can lead to the discovery of new potent VDAs. Herein, we report the total synthesis and biological evaluation of OXi8006 and a diphenolic derivative. Furthermore, the preparation of advanced intermediates en route to future diversely functionalized analogues is presented.

APPROVED BY DIRECTOR OF HONORS THESIS:

---

Dr. Kevin G. Pinney, Department of Chemistry

APPROVED BY THE HONORS PROGRAM:

---

Dr. Andrew Wisely, Director

Date: \_\_\_\_\_

Structural Modifications of OXi8006 Leading to New Indole-Based Anti-Cancer Agents

A Thesis Submitted to the Faculty of  
Baylor University  
In Partial Fulfillment of the Requirements for the  
Honors Program

By  
Priscilla Soth Hor

Waco, Texas

May 2012

## TABLE OF CONTENTS

List of Figures	iii
List of Schemes	iv
List of Abbreviations	v
Chapter One: Introduction	1
Tumor Vasculature	1
Vascular Targeting Therapy	2
Tubulin-Microtubule Protein System	4
Combretastatin	5
VDA Research Design	7
Chapter Two: Materials and Methods	9
General Section	9
Synthesis of OXi8006	9
Synthesis of OXi8006 Analogues	15
Chapter Three: Results and Discussion	19
Synthesis of OXi8006	19
Synthesis of diphenolic derivative <b>13</b>	20
Biochemical Evaluation of <b>13</b>	21
Future Studies	22
Chapter Four: Conclusion	25
Appendix : Selected NMR Spectra	26
References	33

## LIST OF FIGURES

Figure	Page
1. Flavonoid-tumor VDAs FAA	3
2. Colchicine	5
3. Small molecule VDAs CA4 and CA1	7
4. OXi8006 and analogues presented in this study	8
5. OXi8006 and compound <b>13</b> cytotoxicity against DU-145 cell lines	22

## LIST OF SCHEMES

Scheme	Page
1. Total Synthesis of OXi8006	19
2. Synthesis of diphenolic derivative <b>13</b>	20
3. Proposed synthesis of quinoline analogue <b>17</b>	22
4. Proposed synthesis of OXi8006 isomer <b>20</b>	23

## LIST OF ABBREVIATIONS

CA1	Combretastatin A-1
CA4	Combretastatin A-4
CA1P	Combretastatin A-1 Phosphate
CA4P	Combretastatin A-4 Phosphate
$\text{CDCl}_3$	Deuterated Chloroform
$(\text{CD}_3)_2\text{CO}$	Deuterated Acetone
$\text{CH}_2\text{Cl}_2$	Dichloromethane
CV	Column Volume
DIPA	Diisopropylamine
DMA	N, N-Dimethylaniline
DMAP	4-Dimethylaminopyridine
DMXAA	5,6-dimethylanthenone-4-acetic acid
DU-145	human prostate cancer cell line
$\text{Et}_3\text{N}$	Triethylamine
EtOAc	Ethyl acetate
FAA	Flavonoid Acetic Acid



g	grams
Hz	Hertz
IC <sub>50</sub>	Inhibitory Concentration 50%
K <sub>2</sub> CO <sub>3</sub>	Potassium Carbonate
LDA	Lithium Diisopropylamide
MeLi	Methylolithium
MHz	Mega Hertz
mL	milliliters
min	minutes
MMPs	matrix metalloproteinases
mM	milliMolar
mmol	millimoles
<i>n</i> -BuLi	<i>n</i> -Butyllithium
NaHCO <sub>3</sub>	Sodium Bicarbonate
Na <sub>2</sub> SO <sub>4</sub>	Sodium Sulfate
PCC	Pyridinium chlorochromate
r.t.	Room Temperature

SAR	Structure-Activity Relationship
TBAF	Tetrabutylammonium Fluoride
TBS	<i>tert</i> -Butyldimethylsilyl
TBSCl	<i>tert</i> -Butyldimethylsilyl chloride
THF	Tetrahydrofuran
TLC	Thin Layer Chromatography
TNF- $\alpha$	Tumor Necrosis Factor $\alpha$
VDAs	Vascular Disrupting Agents
VEGF	Vascular Endothelial Growth Factor
$^1\text{H}$ NMR	Proton Nuclear Magnetic Spectroscopy
$^{13}\text{C}$ NMR	Carbon Nuclear Magnetic Spectroscopy
Å	Angstrom
°C	Degrees Celsius
$\mu\text{M}$	microMolar

## CHAPTER ONE

### Introduction

#### *Tumor Vasculature*

The circulatory network is a transport mechanism that provides tissues with crucial nutrients while removing waste and excess fluid. For normal tissues, the vascular network is organized and efficient. Blood vessels are regulated by the balance of pro-angiogenic and anti-angiogenic factors and systematic lymphatic vessels that extract waste and fluid.<sup>1</sup> The resulting microvasculature environment is composed of a fully differentiated and evenly distributed network of arterioles, capillaries, and venules that allow sufficient exchange of oxygen and nutrients.

Abnormal tissues, such as tumors, overexpress pro-angiogenic factors resulting in a tortuous, chaotic vasculature. Tumor vasculature is distinguished from normal vasculature in several aspects. Unlike normal vasculature, tumor vasculature consists of blood vessels that are immature, disorganized, and hyperpermeable.<sup>2</sup> Compared to normal vasculature, the tumor microvessels, tumors are highly disordered. Arterioles, capillaries, and venules cannot be distinguished from one another. Vessels often end abruptly and do not exhibit a consistent diameter or shape.<sup>3</sup> As a result of vessel malformation, the amount of nutrients delivered and waste products removed in the tumor environment are drastically reduced. In addition, the irregular vessel shape impairs blood flow to the tumor. Consequently, tumors are often marked by necrotic centers and hypoxic environments.<sup>4</sup>

## *Vascular Targeting Therapy*

Fundamental differences between tumor and normal vasculature offer a selective tactic for anti-cancer therapy.<sup>5</sup> By targeting tumor vasculature, researchers have developed two modes of cancer intervention. The first approach, anti-angiogenesis, seeks to impede tumor neovascularization.<sup>6</sup> The second, vascular disrupting agents, directly targets established tumor vasculature.<sup>7</sup>

Angiogenesis is the formation of new vasculature. During angiogenesis, endothelial cells are activated to express matrix metalloproteinases (MMPs) which degrade the basement membrane of existing vasculature to initiate the formation of new vessels.<sup>8</sup> Antiangiogenic agents prevent neovascularization by inhibiting pro-angiogenic factors and their receptors. A prime target for antimitotic agents is vascular endothelial growth factor (VEGF). VEGF is a pro-angiogenic factor that is over-expressed by most solid tumors.<sup>9</sup> VEGF stimulates the formation of new blood vessels by interacting with specific receptors located on endothelial cells to initiate growth and differentiation of new blood vessels. By inhibiting pro-angiogenic factors, neovascularization is hindered and tumor growth is arrested. The effect prevents metastatic invasion and leads to a cytostatic environment which stabilizes the disease and can lead to tumor dormancy.<sup>10</sup>

Unlike anti-angiogenic agents, small molecule Vascular Disrupting Agents (VDAs) target existing tumor vasculature. VDAs selectively disrupt established tumor vasculature resulting in blood flow occlusion and eventually tumor necrosis. A reduction in blood flow denies tumors of oxygen and nutrients. Extended occlusion leads to substantial tumor necrosis and hypoxia.<sup>11</sup> VDAs utilize physiological differences in tumor endothelial tissue. Tumor endothelial tissue is characterized by increased proliferation

and permeability. Furthermore, tumor endothelium is immensely dependent on its tubulin cytoskeletal infrastructure.<sup>12</sup> Currently, there are two classes of vascular disrupting agents. The first class, flavonoid tumor-VDA, directly disrupt tumor vasculature by selectively inducing apoptosis in vascular endothelial cells.<sup>13</sup> The second class, tubulin-binding agents, selectively target endothelial cells by inducing microtubule depolymerization.<sup>14</sup>

Flavone acetic acid (FAA) is a synthetic flavonoid that displays high activity against tumors.<sup>15</sup> A more promising flavone derivative is 5,6-dimethylanthenone-4a-acetic acid (DMXAA) (Figure 1). This flavonoid tumor-VDA induces tumor vasculature collapse by inducing cytokine factors such as Tumor Necrosis Factor  $\alpha$  (TNF- $\alpha$ ). TNF- $\alpha$  is a necrosis factor overexpressed in tumor endothelial cells.<sup>16</sup> When TNF- $\alpha$  is released from endothelial cells, it binds to tumors resulting in hyperpermeability, extravasation of blood cells, and massive tumor hemorrhagic necrosis of the tumor.<sup>17</sup>

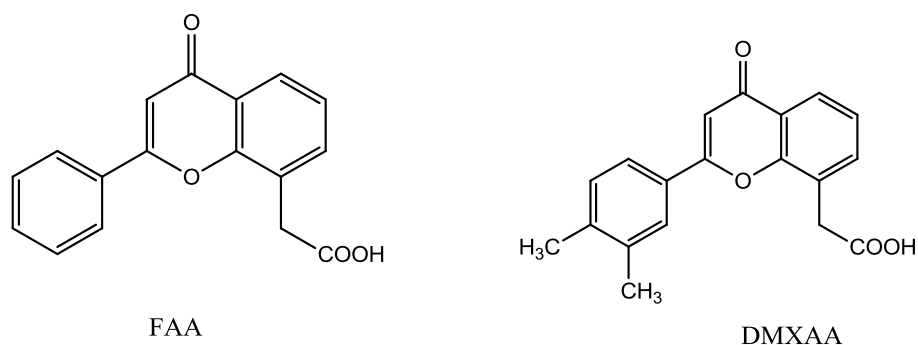


Figure 1: Flavonoid-tumor VDAs FAA and DMXAA

As mentioned earlier, tumor endothelial cells have structural differences from normal vascular endothelium. Tumor endothelial cells are proliferative and depend highly on the tubulin cytoskeletal groundwork.<sup>18</sup> Tubulin binding agents bind to specific sites on tubulin to induce cytoskeletal collapse. By inhibiting tubulin polymerization, the blood

vessel structure degrades leading to vessel occlusion and ultimately, tumor necrosis and hypoxia. One of the lead tubulin-binding agents is combretastatin A-4 (CA4). CA4 belongs to a family of anti-mitotic agents isolated from the South African willow tree *Cambretum caffrum*.<sup>19</sup> CA4 is currently the most potent tubulin-binding agents, with an  $IC_{50}$  of approximately 1.1  $\mu M$ .<sup>20</sup>

#### *Tubulin-Microtubule Protein System*

All blood vessels have an endothelium. The endothelium is composed of endothelial cells that are responsible for extending and remodeling vasculature.<sup>21</sup> Thus, without endothelial cells, blood supply is not possible. Although tumor vasculature is immature and indistinguishable, all the vessels contain proliferative endothelial cells. Since tumor endothelial cells are excessively proliferating, they are highly dependent on the tubulin cytoskeleton. The critical role of the tubulin-microtubule protein system for cell growth makes them a valuable target for anticancer therapy.<sup>22</sup>

Endothelial cells are composed of microtubules. Microtubules are components that contribute to the cell cytoskeleton. Microtubule formation involves two stages: nucleation and elongation. During nucleation,  $\alpha$  and  $\beta$ - tubulin polymerize to form a heterodimer.<sup>23</sup> Afterwards, the tubulin dimer enters the elongation stage by attaching to other dimers via GTP hydrolysis. The resulting protofilaments assemble to form a microtubule. Each microtubule is ring shaped and consists of thirteen tubulin protofilaments.

Microtubules consist of two non-equilibrium dynamics that require GTP hydrolysis. The first state is called dynamic instability. Dynamic instability is a process in which each microtubule end transits between polymerization and depolymerization

phases.<sup>24</sup> Microtubules have two distinct ends called the plus and minus end. The plus end polymerizes and depolymerizes more rapidly than the minus end. Generally, microtubules polymerizes until it changes into a rapid disassembly phase called catastrophe. Catastrophe is followed by a recovery phase in which normal growth is resumed.<sup>25</sup> The second state is called treadmilling. Treadmilling is the net polymerization at one microtubule end balanced by a net depolymerization at the opposite end. Precisely, it involves the movement of tubulin subunits from the plus end of the microtubule to the minus end.<sup>26</sup>

The tubulin-microtubule protein system has three binding sites (taxol, colchicine, and vinblastine) that have been explored for drug development. The taxol site is located on the microtubule polymer, whereas the vinblastine and colchicine sites are located on the tubulin heterodimer. Binding to the taxol site stimulates tubulin stabilization and interferes with tubulin dynamics by enhancing polymerization.<sup>27</sup> Binding to either the vinblastine or colchicine sites induces tubulin depolymerization.<sup>28</sup> This research focuses on developing small molecules that bind to the colchicine site.

### *Combretastatin*

The colchicine site is named after colchicine, the first tubulin binding drug (Figure 2). Despite its high potency against tubulin polymerization, colchicine was too cytotoxic to use as a VDA.<sup>29</sup>

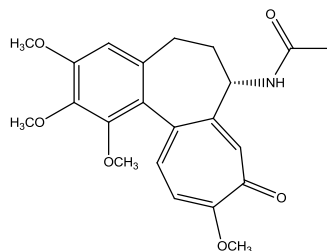


Figure 2: Colchicine

In the late 1970's, George Pettit and colleagues isolated a family of combretastatins from the South African Bushwillow tree *Combretum caffrum*.<sup>30</sup> The family consists of twenty-one compounds that exhibit antimitotic activity. The combretastatin family is structurally similar to colchicine because of the two aryl rings tilted 50-60°.<sup>31</sup> Of the twenty-one compounds, only combretastatin A-1 (CA1) and combretastatin A-4 (CA4) entered clinical trials as VDAs (Figure 3).<sup>32</sup> Of the two, CA4 is the compound of interest for this study. CA4 has an IC<sub>50</sub> of approximately 1.1 μM against tubulin polymerization. In addition, CA4 demonstrates effective cytotoxicity levels against certain cancer cell lines.<sup>20</sup> In order to increase the solubility of CA4 and CA1, soluble analogs CA4P and CA1P were developed.<sup>21</sup> The prodrugs consist of phosphate salts located at the hydroxyl positions. The prodrugs are cleaved by a phosphatase which releases the VDA to act on tubulin. Following the CA4 structure, the phenyl rings are identified as having an A-ring and B-ring. The A-ring coincides with the 3,4,5-trimethoxy motif and the B-ring is representative of the 3'-hydroxy 4'-methoxy phenyl substituents.



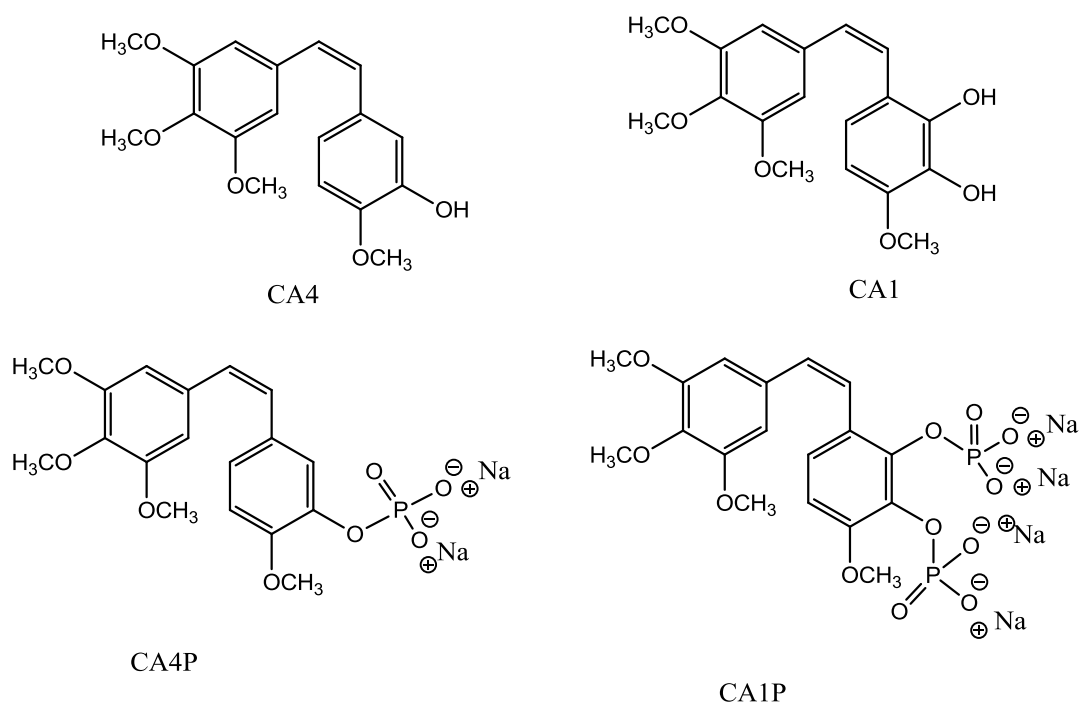


Figure 3: Small molecule VDAs CA4 and CA1 and their corresponding phosphates CA4P and CA1P

#### *VDA Research Design*

The potency of CA4 and CA1 encouraged advanced structure-activity relationship (SAR) studies of the combretastatin family. The SAR studies revealed important pharmacophores required for binding to tubulin at the colchicine site.<sup>28</sup> These pharmacophores include the trimethoxy unit of the A ring, cis-configuration, presence of a methoxy group at the 4-position of the B ring, and the distance between the two aromatic rings.<sup>33-35</sup>

Based on the SAR studies, Pinney group members have synthesized other heterocyclic scaffolds analogs to CA4.<sup>36</sup> The heterocyclic scaffold of interest to this work is the indole scaffold. The similarity of the indoles to the combretastatins is attributed to the similar aryl A-B centroid-to-centroid distances, which are 4.87 Å and 4.88 Å. have been synthesized by Dr. Pinney and co-workers.<sup>29</sup> Furthermore, the indole of primary

interest to this research is OXi8006. OXi8006 is an indole derived VDA previously synthesized by former Pinney group members that exhibits comparable inhibition of tubulin polymerization and demonstrates strong cytotoxicity against human cancer cell lines. Specifically, OXi8006 inhibits tubulin polymerization with an  $IC_{50}$  value of 1-2  $\mu M$ .<sup>29</sup>

In addition to presenting the total synthesis of OXi8006, an additional diphenolic derivative was synthesized and evaluated for cytotoxicity against a prostate cancer cell line. Furthermore, two new analogs of OXi8006 are presented for future synthesis in an ongoing effort to discover new, more potent VDAs.<sup>40</sup> The molecules prepared in this study are illustrated in Figure 4.

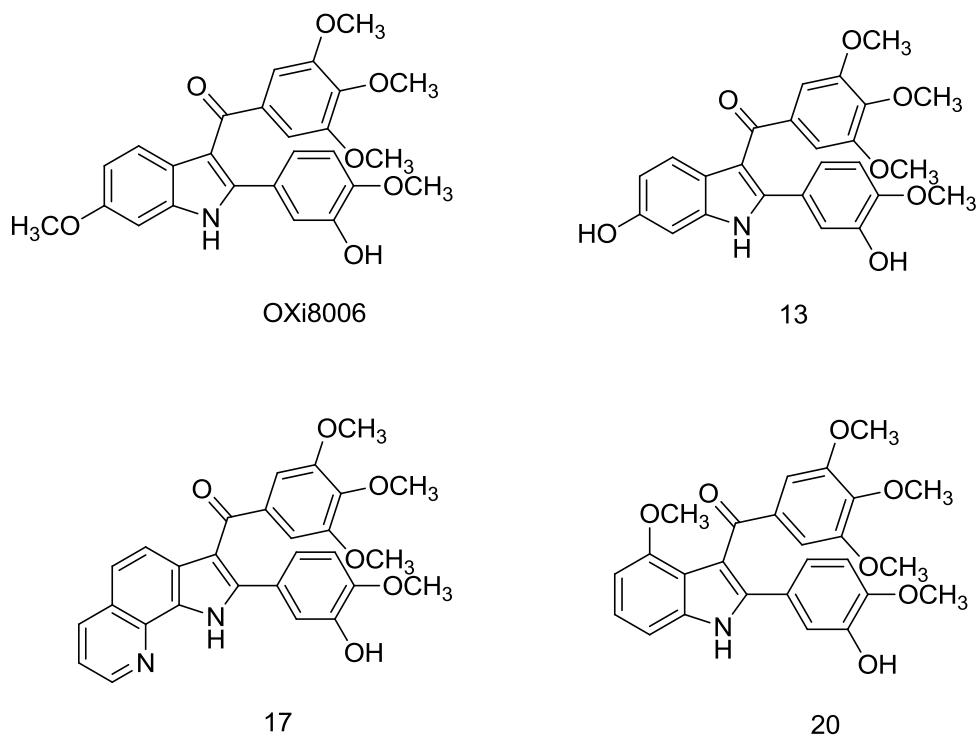


Figure 4: OXi8006 and analogues presented in this study

## CHAPTER TWO

### Materials and Methods

#### *General Section*

All reactions were performed under an inert atmosphere using nitrogen gas unless indicated otherwise. Chemical reagents utilized in the synthetic procedures were obtained from various chemical companies. The silica gel used for flash column chromatography (200-400 mesh, 60 Å) was purchased from Silicycle. Thin layer chromatography (TLC) glass plates pre-coated with silica gel (60 F254, 0.25 mm thickness) were used to monitor reactions. Intermediates and final products were characterized by  $^1\text{H}$  NMR and  $^{13}\text{C}$  NMR using a Varian 500 MHz NMR instrument. TMS was used as an internal standard for spectra recorded in  $\text{CDCl}_3$  or  $(\text{CD}_3)_2\text{CO}$ . All chemical shifts are presented in ppm ( $\delta$ ), peak patterns are noted as broad (br), singlet (s), doublet (d), triplet (t), double doublet (dd) or multiplet (m), and coupling constants ( $J$ ) are expressed in Hz.

#### *Synthesis of OXi8006*

##### *3-(tert-Butyldimethylsilyloxy)-4-methoxybenzaldehyde 2*

To a round bottom flask, 3-hydroxy-4-methoxybenzaldehyde **1** (1.00 g, 6.58 mmol) was dissolved in  $\text{CH}_2\text{Cl}_2$  (18 mL). The solution was then cooled to 0 °C and  $\text{Et}_3\text{N}$  (0.99 mL, 7.2 mmol) was added followed by the addition of DMAP (0.080 g, 0.658 mmol). The reaction mixture was stirred for 10 min. TBSCl (1.09 g, 7.24 mmol) was then added and the solution was stirred for 12 hours allowing the reaction mixture to reach room temperature. Upon completion, the reaction mixture was quenched with water (20 mL) transferred to a separatory funnel and extracted with  $\text{CH}_2\text{Cl}_2$ . The organic

layers were combined, dried over Na<sub>2</sub>SO<sub>4</sub>, filtered, and concentrated under reduced pressure. The TBS-benzaldehyde product **2** (1.1635 g, 4.3673 mmol, 66%) was obtained as a tan oil and was taken to the next step without further purification.

**<sup>1</sup>H NMR** (CDCl<sub>3</sub>, 500 MHz): δ 9.80 (s, 1H, CHO), 7.45 (dd, *J* = 8.5 Hz, *J* = 2.0 Hz, 1H, ArH), 7.35 (d, *J* = 2.0 Hz, 1H, ArH), 6.93 (d, *J* = 8.5 Hz, 1H, ArH), 3.87 (s, 3H, OCH<sub>3</sub>), 0.99 (s, 9H, C(CH<sub>3</sub>)<sub>3</sub>), 0.16 (s, 6H, Si(CH<sub>3</sub>)<sub>2</sub>).

**<sup>13</sup>C NMR** (CDCl<sub>3</sub>, 125 MHz): δ 190.2, 156.2, 145.2, 130.0, 126.0, 119.4, 110.9, 55.1, 25.3, 18.0, -5.0.

*3-(tert-Butyldimethylsilyloxy)-1-(1'-hydroxyethyl)-4-methoxybenzene 3*

TBS protected aldehyde **2** (1.1635 g, 4.3719 mmol) was dissolved in THF (12.9 mL) and the solution was cooled to 0 °C. MeLi (3.57 mL, 5.68 mmol) was then added drop wise and the solution was stirred for 12 hours allowing the mixture reach room temperature. Upon completion, the mixture was quenched with water (15 mL), transferred to a separatory funnel and extracted with EtOAc. The combined organic layers were collected, dried over Na<sub>2</sub>SO<sub>4</sub>, filtered, and concentrated under reduced pressure. TBS protected alcohol **3** (0.9424 g, 3.3365 mmol, 76%) was obtained as a yellow oil and taken to the next step without further purification.

**<sup>1</sup>H NMR** (CDCl<sub>3</sub>, 500 MHz): δ 6.88 (m, 2H, ArH), 6.83 (d, *J* = 8.1 Hz, 1H, ArH), 4.81 (q, *J* = 6.3 Hz, 1H, CH), 3.79 (s, 3H, OCH<sub>3</sub>), 1.82 (s, 1H, OH), 1.45 (d, *J* = 6.3, 3H, CH<sub>3</sub>), 0.99 (s, 9H, (CH<sub>3</sub>)<sub>3</sub>), 0.15 (s, 6H, Si(CH<sub>3</sub>)<sub>2</sub>).

**<sup>13</sup>C NMR** (CDCl<sub>3</sub>, 125 MHz): δ 149.7, 144.5, 138.9, 118.4, 118.0, 117.7, 69.1, 55.1, 25.5, 24.9, 18.2, -4.8.

*3-(tert-Butyldimethylsilyloxy)-4-methoxyacetophenone 4*

Crude TBS protected alcohol **3** (0.9424 g, 3.3365 mmol) was dissolved in CH<sub>2</sub>Cl<sub>2</sub>. After the solution was reduced to 0 °C, Celite (2.0 g) was added and stirred for 10 min. PCC (0.7911 g, 3.6701 mmol) was then added in portions and the mixture was allowed to reach room temperature for 12 hours. Upon completion, the reaction was filtered with celite and silica gel (50/50) plug using CH<sub>2</sub>Cl<sub>2</sub>. The filtrate was then concentrated under reduced pressure to afford the acetophenone product **4** (0.9070 g, 3.2343 mmol, 97%) as a yellow solid which was taken to the next step without further purification.

**<sup>1</sup>H NMR** (CDCl<sub>3</sub>, 500 MHz): δ 7.57 (dd, *J* = 2.0 Hz, 8.5 Hz, 1H, ArH), 7.46 (d, *J* = 2.0 Hz, 1H, ArH), 6.86 (d, *J* = 8.5 Hz, 1H, ArH), 3.86 (s, 3H, OCH<sub>3</sub>), 2.52 (s, 3H, CH<sub>3</sub>), 1.00 (s, 9H, C(CH<sub>3</sub>)<sub>3</sub>), 0.16 (s, 6H, Si(CH<sub>3</sub>)<sub>2</sub>).

**<sup>13</sup>C NMR** (CDCl<sub>3</sub>, 125 MHz): δ 196.7, 155.3, 144.8, 130.5, 123.5, 120.4, 110.7, 55.4, 26.2, 25.6, 18.4, -4.7.

*1-(3-tert-Butyldimethylsilyloxy-4-methoxyphenyl)-1-trimethylsilyl ethene 5*

To a solution of diisopropylamine (0.683 mL, 4.845 mmol) dissolved in THF (9.69 mL) at 0 °C, *n*-BuLi (1.94 mL, 4.845 mmol) was added dropwise. The reaction mixture was stirred for 15 min upon which TBS-acetophenone **4** (0.9070 g, 3.2343 mmol) dissolved in THF was added dropwise and the solution was stirred for an

additional 15 min. TMSCl (0.616 mL, 4.845 mmol) was added slowly and the reaction mixture was allowed to reach room temperature over 3 hours. Upon completion, the reaction was quenched with 10% NaHCO<sub>3</sub> and transferred to a separatory funnel to be extracted with hexanes and dried over K<sub>2</sub>CO<sub>3</sub>. The combined organic layers were filtered and concentrated under reduced pressure to afford the TMS enol ether **5** (1.7 g, 4.8 mmol, 30%) as a dark yellow oil and was taken to the next step without further purification.

**<sup>1</sup>H NMR** (CDCl<sub>3</sub>, 500 MHz): δ 7.18 (dd, *J* = 2.5 Hz, 8.5 Hz, 1H ArH), 7.12 (d, *J* = 2.5 Hz, 1H, ArH), 6.80 (d, *J* = 8.5 Hz, 1H, ArH), 4.78 (d, *J* = 1.5 Hz, 1H, CH<sub>2</sub>), 4.34 (d, *J* = 1.5 Hz, 1H, CH<sub>2</sub>), 3.81 (s, 3H, OCH<sub>3</sub>), 1.03 (s, 9H, C(CH<sub>3</sub>)<sub>3</sub>), 0.27 (s, 9H, Si(CH<sub>3</sub>)<sub>3</sub>), 0.18 (s, 6H, Si(CH<sub>3</sub>)<sub>2</sub>).

**<sup>13</sup>C NMR** (CDCl<sub>3</sub>, 125 MHz): δ 155.3, 151.1, 144.4, 130.6, 118.8, 118.1, 111.2, 89.5, 55.4, 25.7, 18.4, 0.03, -4.7).

*3'-(tert-Butyldimethylsilyloxy)-4'-methoxy-2-bromoacetophenone 6*

To a solution of TMS enol ether (1.7 g, 4.8 mmol) dissolved in CH<sub>2</sub>Cl<sub>2</sub> (14.4 mL), K<sub>2</sub>CO<sub>3</sub> (0.028 g, 0.2045 mmol) was added. The solution was then cooled to 0°C and Br<sub>2</sub> (0.15 mL, 2.89 mmol) was added drop wise and the reaction mixture was stirred for 30 min. The mixture was monitored by TLC every 30 minutes until the reaction went to completion. After which, the reaction was quenched with a solution of 10% Na<sub>2</sub>S<sub>2</sub>O<sub>2</sub>. The solution was transferred to a separatory funnel, extracted with CH<sub>2</sub>Cl<sub>2</sub>, and concentrated under reduced pressure. The crude mixture was then subjected to column chromatography eluting with 10% (3 x 100 mL), 20% (3 x 100 mL), and 30% (3 x 100

mL) EtOAc-hexanes while monitoring by TLC affording the bromoacetophenone product **6** (0.13 g, 0.36 mmol, 30%) as a tan red solid.

**<sup>1</sup>H NMR** (CDCl<sub>3</sub>, 500 MHz): δ 7.61 (dd, *J*=2.5 Hz, 8.5 Hz, 1H, ArH), 7.48 (d, *J*=2.5 Hz, 1H, ArH), 6.88 (d, *J*=8.5 Hz, 1H, ArH), 4.37 (s, 2H, CH<sub>2</sub>), 3.88 (s, 3H, OCH<sub>3</sub>), 1.00 (s, 9H, C(CH<sub>3</sub>)<sub>3</sub>), 0.17 (s, 6H, Si(CH<sub>3</sub>)<sub>2</sub>).

**<sup>13</sup>C NMR** (CDCl<sub>3</sub>, 125 MHz): δ 189.8, 156.1, 145.1, 127.1, 124.2, 121.0, 111.0, 55.5, 30.6, 25.6, 18.4, -4.6.

*2-(3'-tert-Butyldimethylsilyloxy-4'-methoxyphenyl)-6-methoxyindole 7*

A solution of *m*-anisidine (0.13 mL, 1.19 mmol) was dissolved in N, N-dimethylaniline (1.08 mL) and heated to reflux at 170 °C. Then a solution of bromoacetophenone **6** (0.13 g, 0.36 mmol) dissolved in EtOAc was added drop wise to the reaction mixture and stirred at 170 °C 12 hours. Upon completion, the reaction was cooled to room temperature and extracted with EtOAc. The combined organic layers were collected, dried over Na<sub>2</sub>SO<sub>4</sub>, filtered, and concentrated under reduced pressure. The crude mixture was then subjected to flash column chromatography eluting with 10% (3 x 100 mL), 20% (3 x 100 mL), and 30% (3 x 100 mL) EtOAc-hexanes solvent while monitoring by TLC to afford indole **7** (0.3647g, 0.9508 mmol, 20%) as a tan yellow solid.

**<sup>1</sup>H NMR** (CDCl<sub>3</sub>, 500 MHz): δ 8.11 (br s, 1H, NH), 7.47 (d, *J*= 8.5 Hz, 1H, ArH), 7.16 (dd, *J*= 2.0 Hz, 8.5 Hz, 1H, ArH), 7.13 (d, *J*= 2.5 Hz, 1H, ArH), 6.90 (d, *J*= 8.5 Hz, 1H, ArH), 6.89 (d, *J*= 2.5 Hz, 1H, ArH), 6.79 (dd, *J*=2.5 Hz, 8.5 Hz, 1H, ArH), 6.64 (dd, *J*=1.0Hz, 2.0Hz, 1H, ArH), 6.79 (dd, *J*= 2.5 Hz, 8.5 Hz, 1H, ArH), 6.64 (dd, *J*= 1.0 Hz,

1H, ArH), 5.79 (dd,  $J=2.5$  Hz, 8.5 Hz, 1H, ArH), 6.64 (dd,  $J=1.0$  Hz, 2.0 Hz, 1H, ArH), 3.86 (s, 3H, OCH<sub>3</sub>), 3.84 (s, 3H, OCH<sub>3</sub>), 1.04 (s, 9H, C(CH<sub>3</sub>)<sub>3</sub>), 0.21 (s, 6H, Si(CH<sub>3</sub>)<sub>2</sub>).

<sup>13</sup>C NMR (CDCl<sub>3</sub>, 125 MHz):  $\delta$  156.3, 150.5, 145.4, 137.4, 136.9, 125.8, 123.7, 120.9, 118.2, 117.8, 112.4, 109.9, 98.6, 94.5, 55.6, 55.4, 25.7, 18.5, -4.6.

*2-(3'-tert-Butylmethylsiloxy-4'-methoxyphenyl-3-(3'',4'',5''-trimethoxybenzoyl)-6-methoxyindole 9*

To a solution of indole **7** (0.545 g, 1.420 mmol) dissolved in *o*-dichlorobenzene (10 mL), 3,4,5-trimethoxybenzoyl chloride **8** (0.4918 g, 2.1300 mmol) was added. The reaction mixture was then heated to reflux at 170 °C for 12 hours. Upon completion excess *o*-dichlorobenzene was removed under reduced pressure and the resulting dark green oil was subjected to column chromatography eluting with 10% (3 x 100 mL), 20% (3 x 100 mL), and 30% (3 x 100 mL) EtOAc-hexanes affording **9** (0.2528 g, 0.4376 mmol, 10%) as a yellow solid.

<sup>1</sup>H NMR (CDCl<sub>3</sub>, 500 MHz):  $\delta$  8.42 (br s, 1H, NH), 7.93 (d,  $J=9.5$  Hz, 1H, ArH), 6.99 (s, 2H, ArH), 6.94 (dd,  $J=2.0$  Hz, 8.0 Hz, 1H, ArH), 6.91 (dd,  $J=2.0$  Hz, 9.0 Hz, 1H, ArH), 6.91 (d,  $J=2.0$  Hz, 1H, ArH), 6.77 (d,  $J=2.0$  Hz, 1H, ArH), 6.70 (d,  $J=8.5$  Hz, 1H, ArH), 3.87 (s, 3H, OCH<sub>3</sub>), 3.79 (s, 3H, OCH<sub>3</sub>), 3.74 (s, 3H, OCH<sub>3</sub>), 3.69 (s, 6H, OCH<sub>3</sub>), 0.94 (s, 9H, C(CH<sub>3</sub>)<sub>3</sub>), 0.04 (s, 6H, Si(CH<sub>3</sub>)<sub>2</sub>).

<sup>13</sup>C NMR (CDCl<sub>3</sub>, 125 MHz):  $\delta$  191.9, 157.4, 152.6, 151.6, 145.2, 142.1, 141.3, 136.5, 134.6, 125.2, 123.4, 122.6, 122.3, 121.9, 112.9, 111.8, 111.7, 107.4, 94.6, 60.9, 56.1, 55.9, 55.5, 25.8, 18.5, -4.7.

*(2-(3-Hydroxy-4-methoxyphenyl)-6-methoxy-1H-indol-3-yl)(3,4,5-trimethoxyphenyl)methanone 10*



To a solution of TBS protected indole (0.500 g, 0.866 mmol) dissolved in THF (10 mL), TBAF (1.0 mL, 0.89 mmol) was added. The solution was then stirred at room temperature for 30 min. Upon completion, the reaction was quenched with water (20 mL), transferred to a separatory funnel and extracted with EtOAc. The organic layers were collected, dried over Na<sub>2</sub>SO<sub>4</sub>, filtered, and concentrated under reduced pressure. The resulting crude mixture was purified by column chromatography eluting with 10% (3 x 100 mL), 20% (3 x 100 mL), and 30% (3 x 100 mL) EtOAc-hexanes affording OXi8006 (0.343 g, 0.7400 mmol, 85%) as a yellow solid.

**<sup>1</sup>H NMR** (CDCl<sub>3</sub>, 500 MHz): δ 8.30 (br s, 1H, NH), 7.93 (d, *J*=9.5 Hz, 1H, ArH), 6.96 (s, 2H, ArH), 6.95 (d, *J*=2.0 Hz, 1H, ArH), 6.93 (dd, *J*=2.5 Hz, 9.5 Hz, 1H, ArH), 6.92 (d, *J*=2.5 Hz, 1H, ArH), 6.78 (dd, *J*=2.0 Hz, 8.0 Hz, 1H, ArH), 6.65 (d, *J*=8.5 Hz, 1H, ArH), 5.55 (s, 1H, OH), 3.89 (s, 3H, OCH<sub>3</sub>), 3.84 (s, 3H, OCH<sub>3</sub>), 3.80 (s, 3H, OCH<sub>3</sub>), 3.7 (s, 6H, OCH<sub>3</sub>).

**<sup>13</sup>C NMR** (CDCl<sub>3</sub>, 125 MHz): δ 192.7, 157.1, 152.5, 147.0, 145.3, 143.3, 141.0, 136.6, 135.0, 125.1, 123.0, 122.1, 121.5, 115.1, 112.6, 111.6, 110.3, 107.4, 94.8, 60.8, 56.0, 55.8, 55.6.

### *Synthesis of OXi8006 Analogues*

*2-(3'-tert-Butyldimethylsiloxy-4'-methoxyphenyl)-3-(3'',4'',5''trimethoxybenzoyl)-6-tert-butyldimethylsiloxyindole* **12**

To a solution of TBS protected indole **11** (0.3444 g, 0.7119 mmol) dissolved in *o*-dichlorobenzene (25 mL), 3,4,5-trimethoxybenzoylchloride (0.25 g, 1.1 mmol) was added. The solution was then heated to reflux at 170 °C for 12 hours. After completion, *o*-dichlorobenzene was removed under reduced pressure and the resulting dark green oil

was subjected to flash column chromatography using a pre-packed 50 g silica column [eluents: solvent A, EtOAc, solvent B, hexanes; gradient, 7% A/93% B (4CV), 7% A/93% B  $\rightarrow$  60% A/40% B (10 CV), 60% A/40% B (2 CV); flow rate, 40 mL/min; monitored at  $\lambda$ 's 254 and 280 nm] resulting in a pale yellow solid product **12** (0.27 g, 0.40 mmol, 20%,  $R_f$  0.33 (70:30 hexanes: EtOAc).

**$^1\text{H}$  NMR** ( $(\text{CD}_3)_2\text{CO}$ , 500 MHz):  $\delta$  8.31 (br s, 1H,  $\text{NH}$ ), 7.90 (d,  $J$  = 8.5 Hz, 1H,  $\text{ArH}$ ), 6.99 (s, 2H,  $\text{ArH}$ ), 6.94 (dd,  $J$  = 2.0 Hz, 8.5 Hz, 1H,  $\text{ArH}$ ), 6.89 (d,  $J$  = 2.0 Hz, 1H,  $\text{ArH}$ ), 6.82 (dd,  $J$  = 2.0 Hz, 8.5 Hz, 1H,  $\text{ArH}$ ), 6.76 (d,  $J$  = 2.5 Hz, 1H,  $\text{ArH}$ ), 6.70 (d,  $J$  = 8.0 Hz,  $\text{ArH}$ ), 3.79 (s, 3H,  $\text{OCH}_3$ ), 3.75 (s, 3H,  $\text{OCH}_3$ ), 3.69 (s, 6H,  $\text{OCH}_3$ ), 1.01 (s, 9H,  $\text{C}(\text{CH}_3)_3$ ), 0.94 (s, 9H,  $\text{C}(\text{CH}_3)_3$ ), 0.22 (s, 6H,  $\text{Si}(\text{CH}_3)_2$ ), 0.04 (s, 6H,  $\text{Si}(\text{CH}_3)_2$ ).

**$^{13}\text{C}$  NMR** ( $(\text{CD}_3)_2\text{CO}$ , 125 MHz):  $\delta$  191.8, 153.0, 152.6, 151.7, 145.2, 142.3, 141.3, 136.5, 134.6, 125.2, 123.9, 122.3, 121.9, 116.7, 112.9, 111.8, 107.4, 105.1, 101.6, 60.9, 56.1, 55.5, 25.9, 25.8, 18.46, 18.45, -.42, -4.8.

*2-(3'-Hydroxy-4'-methoxyphenyl)-3-(3'',4'',5''trimethoxybenzoyl)-6-hydroxyindole* **13**

To a solution of di-TBS protected indole **12** (0.4001 g, 0.5901 mmol) dissolved in THF (10 mL), TBAF (1.0 mL, 0.89 mmol) was added. The solution was then stirred at room temperature for 30 min. Upon completion, the reaction was quenched with water (10 mL) and transferred to a separatory funnel to be extracted with EtOAc. The combined organic layers were collected, dried over  $\text{Na}_2\text{SO}_4$ , filtered, and concentrated under reduced pressure. The resulting crude solution was purified by flash column chromatography using a prepacked 50 g silica column [eluents: solvent A, EtOAc, solvent B, hexanes; gradient, 12% A/88% B (4CV), 12% A/88% B  $\rightarrow$  100% A/0% B (10

CV), 100% A/0% B (1.4 CV); flow rate, 40 mL/min; monitored at  $\lambda$ 's 254 and 280 nm] resulting in the diphenolic indole product **13** (0.1111 g, 0.2472 mmol, 42%) as a yellow powder.

**<sup>1</sup>H NMR** (CDCl<sub>3</sub>, 500 MHz):  $\delta$  11.62 (br s, 1H, NH), 9.19 (br s, 1H, OH), 9.00 (br s, 1H, OH), 7.66 (d,  $J$  = 8.5 Hz, 1H, ArH), 6.82 (d,  $J$  = 2.0 Hz, 1H, ArH), 6.78 (s, 2H, ArH), 6.74 (d,  $J$  = 9.0 Hz, 2H, ArH), 6.67 (t,  $J$  = 2.5 Hz, 1H, ArH), 6.65 (t,  $J$  = 3.0 Hz, 1H, ArH), 3.69 (s, 3H, OCH<sub>3</sub>), 3.61 (s, 6H, OCH<sub>3</sub>), 3.59 (s, 3H, OCH<sub>3</sub>).

**<sup>13</sup>C NMR** (CDCl<sub>3</sub>, 125 MHz):  $\delta$  192.0, 155.2, 153.4, 148.5, 147.0, 143.7, 141.8, 38.0, 136.4, 126.5, 123.4, 122.7, 122.0, 116.9, 113.1, 112.3, 111.8, 106.0, 97.4, 60.4, 56.2

*2-(3-((tert-butyldimethylsilyl)oxy)-4-methoxyphenyl)-1H-pyrrolo[3,2-h]quinoline* **15**

Quinoline **14** (1.324 g, 9.184 mmol) was dissolved in N, N dimethylaniline (24 mL), and the reaction mixture was heated to 170 °C. Once at reflux, bromoacetophenone **5** (1.0 g, 2.8 mmol) dissolved in EtOAc was added dropwise to the mixture and stirred at reflux 12 hours. Upon completion, the reaction was quenched cooled to room temperature, transferred to a separatory funnel and extracted with EtOAc. The combined organic layers were collected, dried over Na<sub>2</sub>SO<sub>4</sub> and concentrated under reduced pressure. The crude mixture was purified by flash column chromatography using a prepacked 50 g silica column [eluents: solvent A, EtOAc, solvent B, hexanes; gradient, 7% A/93% B (4CV), 7% A/93% B  $\rightarrow$  60% A/40% B (10 CV), 60% A/40% B (5.2 CV); flow rate, 40 mL/min; monitored at  $\lambda$ 's 254 and 280 nm] resulting in product **15** (0.0889 g, 0.2197, 8%) as a dark brown oil.

**$^1\text{H}$  NMR** ( $\text{CDCl}_3$ , 500 MHz):  $\delta$  10.36 (br s, 1H,  $\text{NH}$ ), 8.78 (dd,  $J=1.5$  Hz, 4.5 Hz, 1H,  $\text{ArH}$ ), 8.21 (dd,  $J=1.0$  Hz, 8.0 Hz, 1H,  $\text{ArH}$ ), 7.77 (d,  $J=8.5$  Hz, 1H,  $\text{ArH}$ ), 7.44 (d,  $J=8.5$  Hz, 1H,  $\text{ArH}$ ), 7.33 (dd,  $J=3.0$  Hz, 2H,  $\text{ArH}$ ), 7.30 (d,  $J=2.0$  Hz, 1H,  $\text{ArH}$ ), 6.90 (d,  $J=8.5$  Hz, 1H,  $\text{ArH}$ ), 6.87 (d,  $J=2.0$  Hz, 1H,  $\text{ArH}$ ), 3.84 (s, 3H,  $\text{OCH}_3$ ), 1.04 (s, 9H,  $\text{C}(\text{CH}_3)_3$ ), 0.21 (s, 6H,  $\text{Si}(\text{CH}_3)_2$ ).

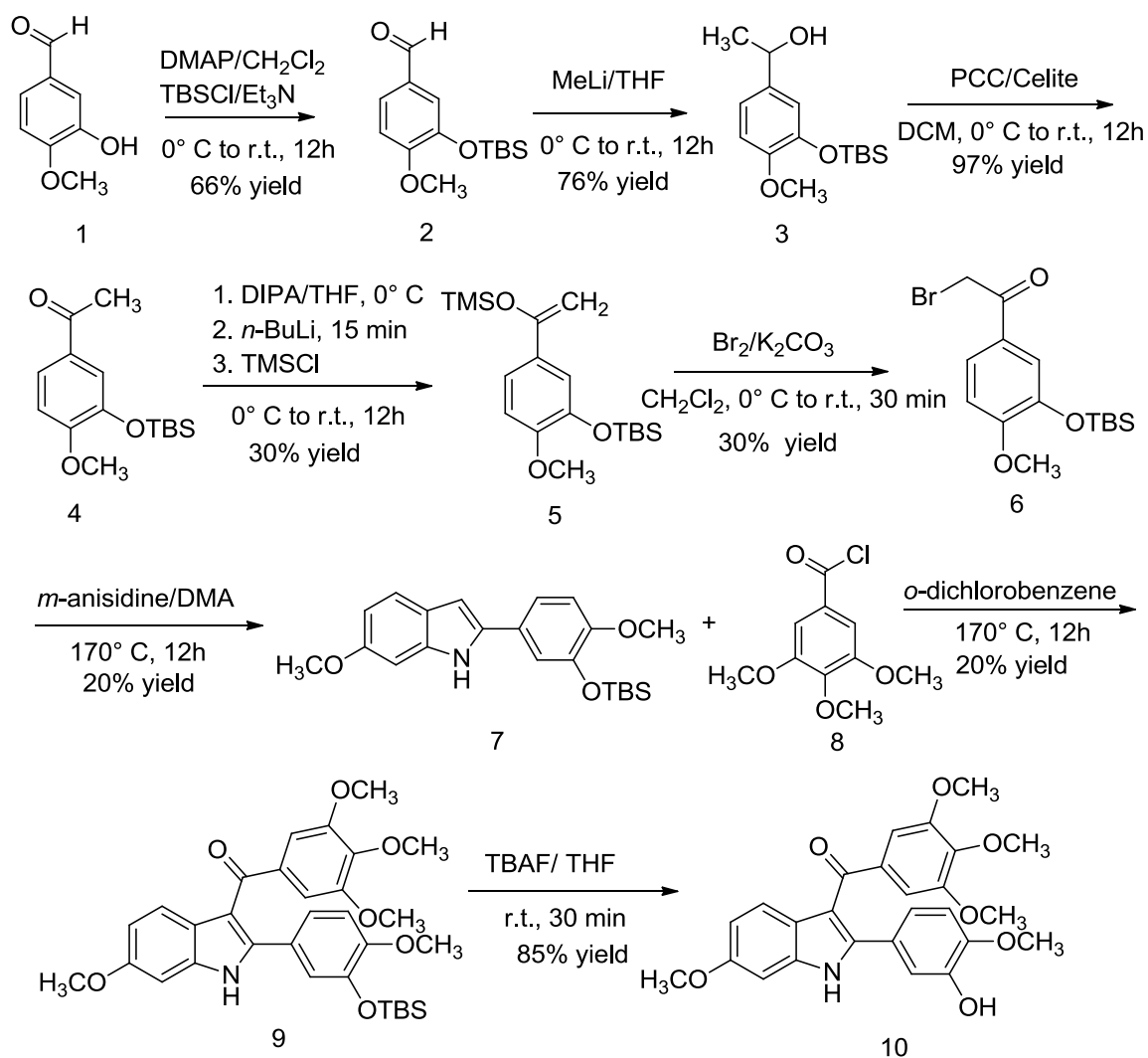
**$^{13}\text{C}$  NMR** ( $\text{CDCl}_3$ , 125 MHz):  $\delta$  151.1, 148.0, 145.6, 138.2, 137.7, 136.9, 131.1, 128.5, 125.5, 125.1, 121.7, 119.8, 119.1, 118.9, 118.4, 112.5, 100.5, 55.6, 25.9, 18.6, -4.4.

## CHAPTER THREE

### Results and Discussion

#### *Synthesis of OXi8006*

A one gram scale synthesis of OXi8006 is illustrated in Scheme 1.



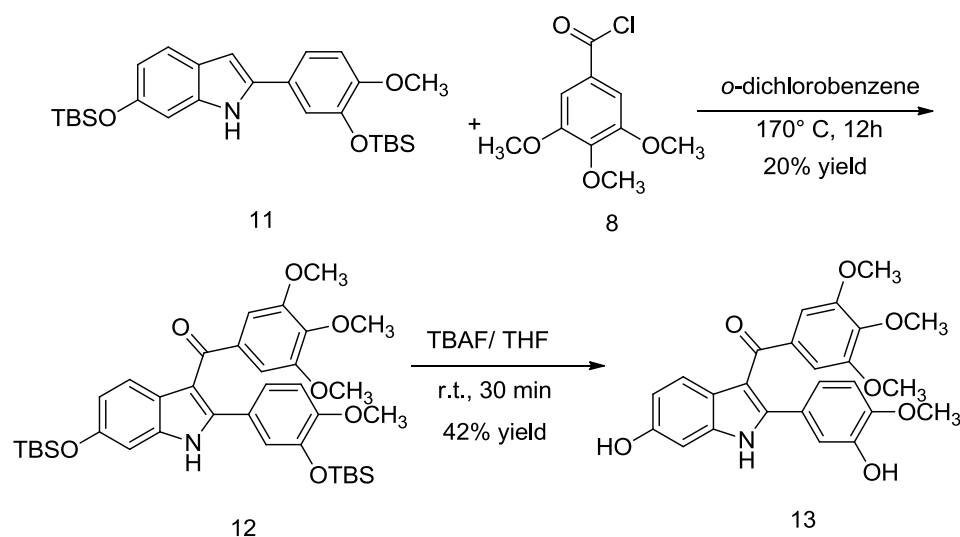
Scheme 1: Total Synthesis of OXi8006

The synthesis towards OXi8006 begins with the TBS protection of commercially available isovanillin to afford silylether aldehyde **2**. This step employs TBSCl, DMAP,

and Et<sub>3</sub>N to protect the phenol of isovanillin. The carbonyl of the desired aldehyde **2** was then treated with MeLi to afford the methylated secondary alcohol **3** which was then subjected to oxidation in the presence of PCC resulting in the desired acetophenone **4**. Celite was to prevent coagulation of PCC. Acetophenone **4** was then subjected to a solution of LDA, generated *in situ*, followed by the addition of TMSCl to afford enol ether **5** which was brominated to obtain bromoacetophenone **6**. Presumably through a Bischler-Mohrlau indole reaction, bromoacetophenone **6** was cyclized to indole **7** in the presence of 3-methoxyaniline and N,N-dimethylaniline.<sup>37-39</sup> Indole **7** was then subjected to a Friedel-Crafts acylation upon treatment with 3,4,5-trimethoxybenzoylchloride resulting in the substituted indole **9**. Upon deprotection of the TBS group from the benzoylated indole **9** with TBAF, OXi8006 **10** was obtained as a yellow powder.

#### *Synthesis of diphenolic derivative 13*

The synthetic route affording the diphenolic derivative **13** is illustrated in Scheme 2.



Scheme 2: 2-(3'-*tert*-Butyldimethylsiloxy-4'-methoxyphenyl)-3-(3'',4'',5''trimethoxybenzoyl)-6-*tert*-butyldimethylsiloxyindole **13**

The advanced protected diphenolic indole **11** intermediate was prepared by Pinney Lab member Matthew MacDonough. Indole **11** was subjected to a Friedel-Crafts acylation in the presence of 3,4,5-trimethoxybenzoylchloride to afford the benzoylated indole **12**. The TBS protecting groups indole of **12** were then cleaved by treatment with a solution of TBAF which provided the desired diphenolic derivative **13**.

#### *Biochemical Evaluation of **13***

OXi8006 and the derived diphenolic derivative **13** were evaluated for their cytotoxicity against the DU-145 cell line through a collaborative effort with the Trawick Group at Baylor University. The IC<sub>50</sub> value of diphenol derivative **13** against the prostate cancer (DU-145) cell line was  $2.77 \pm 0.14 \mu\text{M}$ . Compared to the IC<sub>50</sub> value of OXi8006, which was  $0.0245 \pm 0.0102 \mu\text{M}$ , the diphenol derivative is not as cytotoxic as OXi8006 against prostate cancer cell lines. This indicates that the presence of the methoxy substituent on the indole ring plays an important role in the cytotoxicity of OXi8006. Although **13** is not as cytotoxic against the DU-145 cell line, further biological evaluation is in progress for the diphenolic derivative. In addition to assessing the cytotoxicity of compound **13** against additional cancer cell lines, **13** will also be evaluated for inhibition of tubulin polymerization.

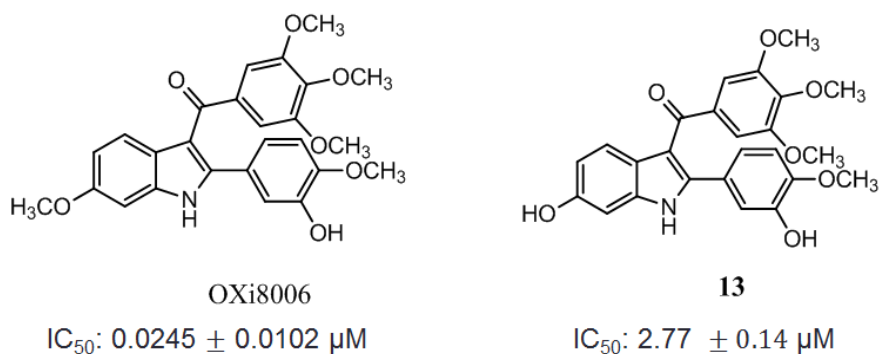
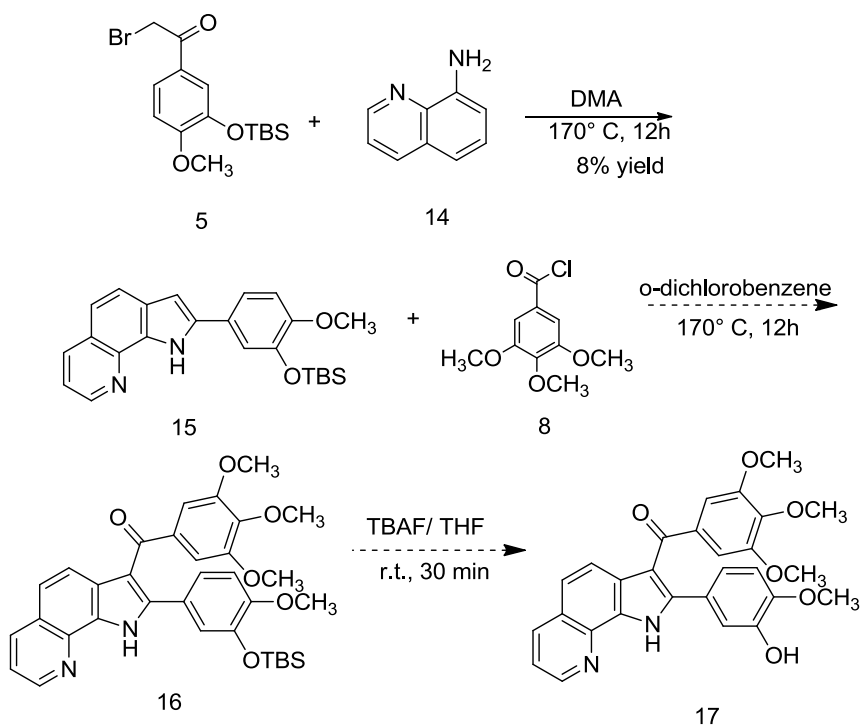


Figure 5: OXi8006 and compound **13** cytotoxicity against the DU-145 cell line

### Future Studies

In pursuit of developing new indole VDAs, two potential analogues as well as their proposed synthesis are presented. The quinoline analogue **17** is illustrated in Scheme 3.

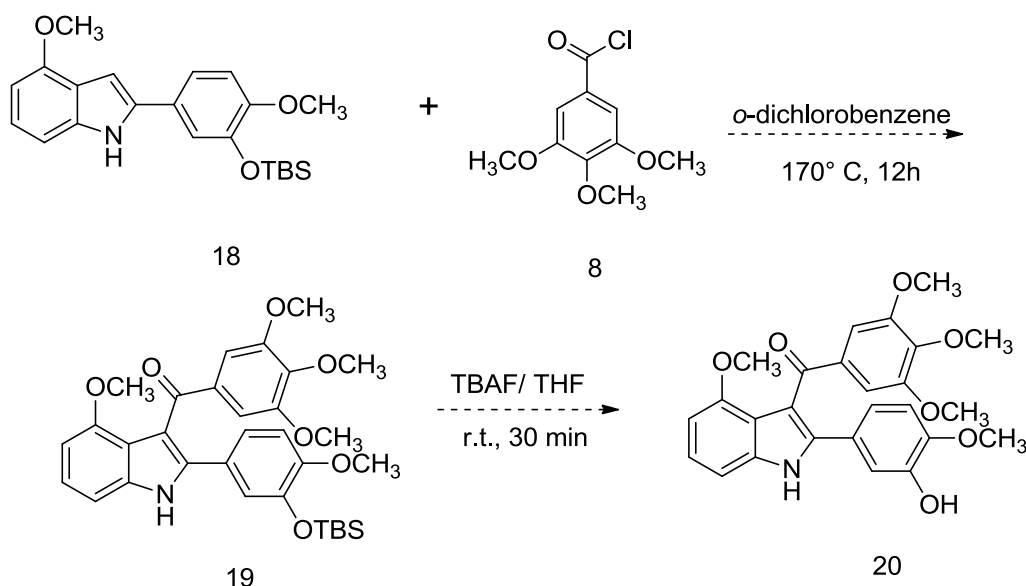


Scheme 3: Proposed Synthesis of 2-(3-((tert-Butyldimethylsilyl)oxy)-4-methoxyphenyl)-1H-pyrrolo[3,2-h]quinoline **17**



The proposed synthesis leading to the quinolone analogue follows a similar route as Scheme 1. Bromoacetophenone **5** was cyclized into indole **15** in the presence of quinoline **14** and N, N-dimethylaniline. Preparation of quinolone analog **17** will proceed to follow Scheme 3, unless modifications of the synthetic route are needed. Compound **17** varies from OXi8006 with the presence of a quinoline located on the indole ring.

In addition to the quinoline analog, a proposed synthesis of an isomer of OXi8006 is presented in Scheme 4.



Scheme 4: Proposed Synthesis of (2-(3-Hydroxy-4-methoxyphenyl)-4-methoxy-1H-indol-3-yl) (3,4,5-trimethoxyphenyl)methanone **20**

The synthetic route leading to the protected indole isomer **18** was accomplished by Pinney Lab member Matthew MacDonough. The proposed synthesis for this indole isomer follows the same route as Scheme 1. Thus far, the indole isomer **18** has been benzoylated with 3,4,5-trimethoxybenzoylchloride. Further purification steps are needed before determining whether product has formed. Compound **20** differs from OXi8006 at

the position of one methoxy group. Unlike OXi8006, the methoxy substituent is located on the fourth position of the indole ring instead of the sixth position.

Once synthesized and biologically evaluated, quinoline **17** and indole isomer **20** may provide insight into substituent effects on the indole core. Furthermore, the analogues will be added to the library of OXi8006 analogues in an ongoing effort to discover new and more potent inhibitors of tubulin polymerization.<sup>40</sup>

## CHAPTER FOUR

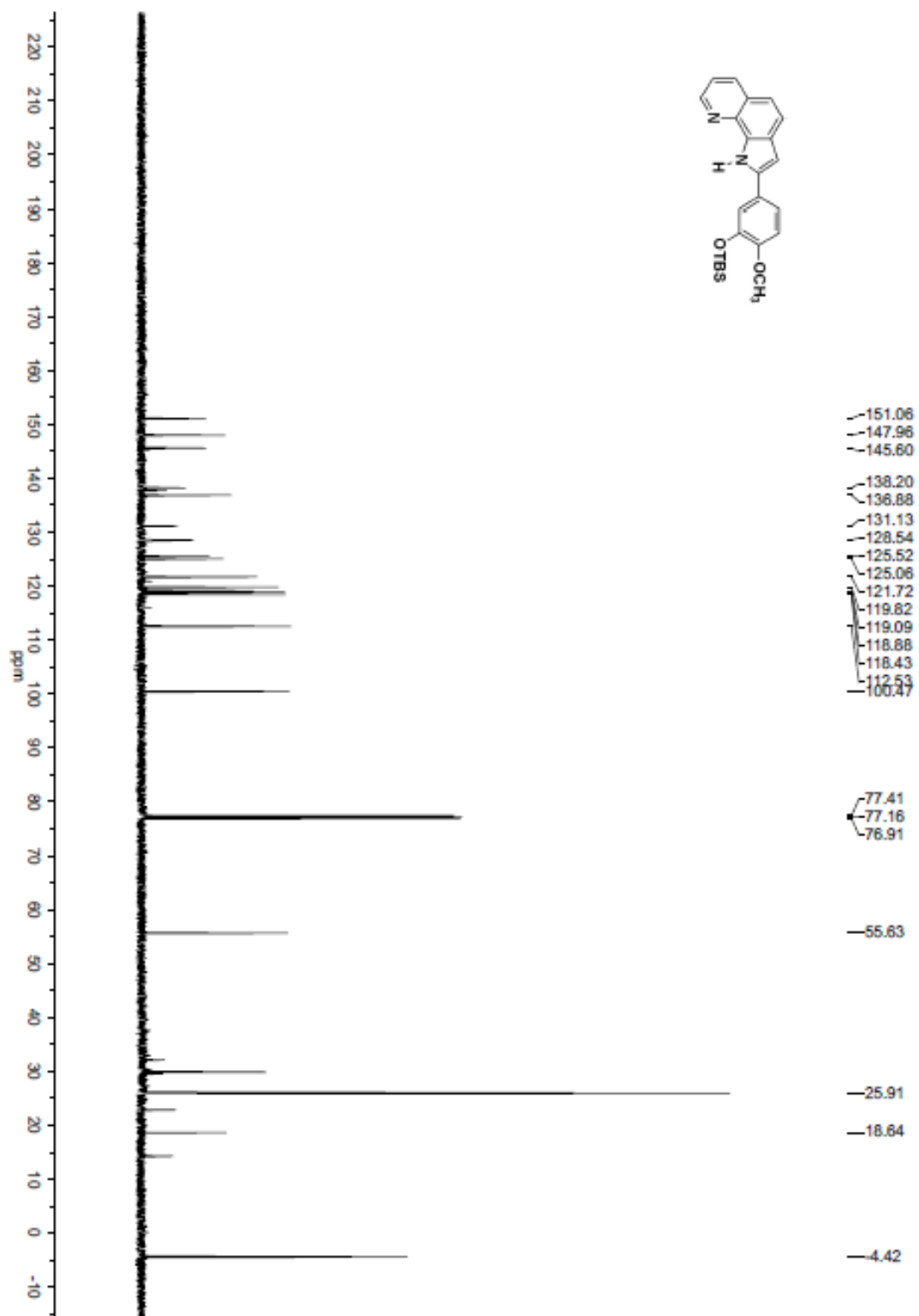
### Conclusion

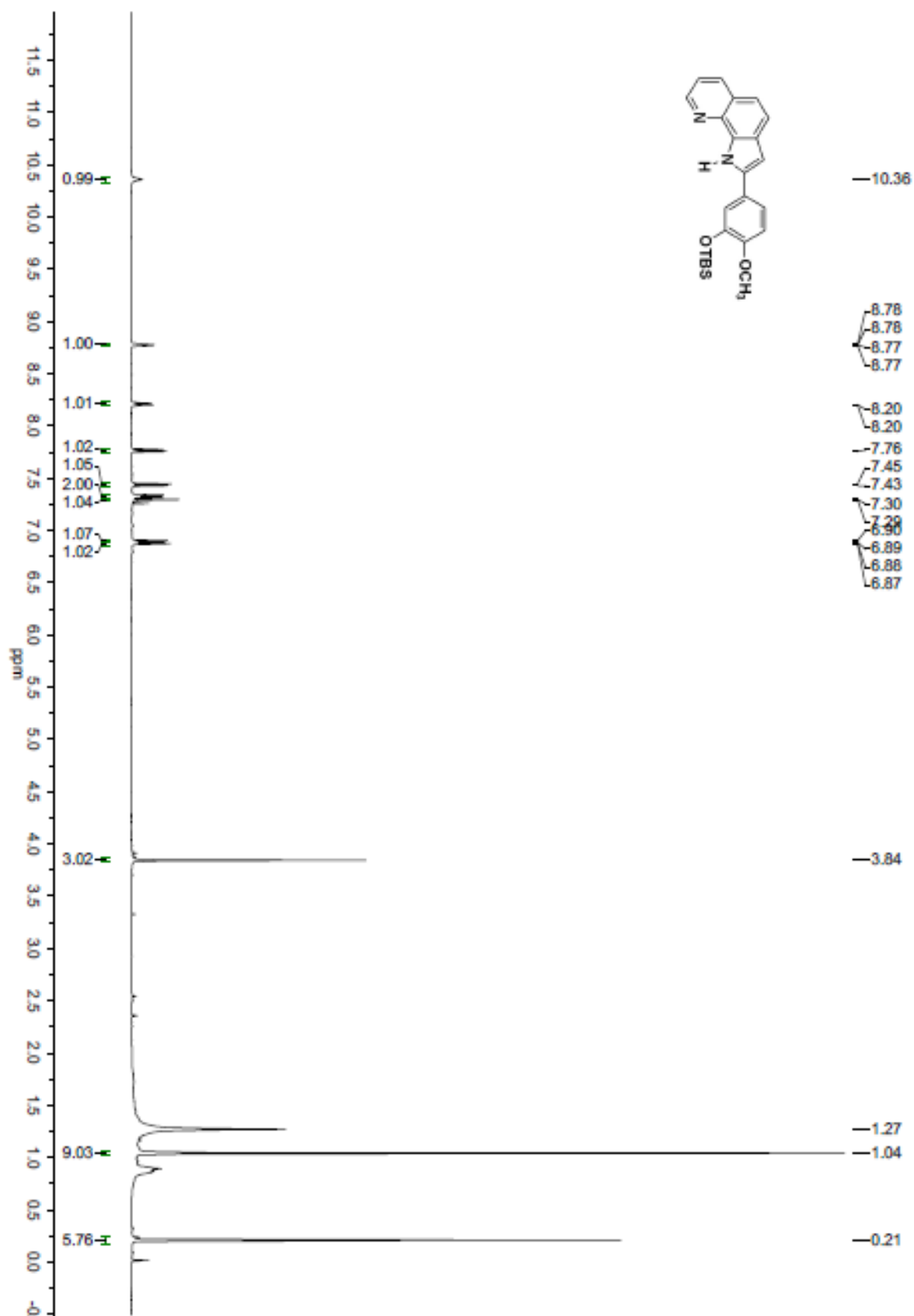
This study resulted in the successful chemical synthesis of OXi8006 and an additional diphenolic derivative. The diphenolic derivative, compound **13**, differs from OXi8006 by only one substituent. Instead of a methoxy group located on the C ring, compound **13** contains a phenolic group. Thus far, **13** has been evaluated for cytotoxicity against DU-145, a prostate cancer cell line. With an  $IC_{50}$  value of  $2.77 \pm 0.14 \mu\text{M}$ , the diphenolic derivative is not as cytotoxic against this prostate cancer cell line as OXi8006 (Figure 5). Nonetheless, this new derivative is valuable for advancing the SAR profile for OXi8006. Currently, the derivative is undergoing evaluation for inhibition against tubulin polymerization and cytotoxicity against other human cancer cell lines. Future studies will involve the synthesis and biological evaluation of compounds **17** and **20**. Overall, the satisfactory yields produced from most of the reactions suggest that this is a valuable synthetic route that can be used to expand the library of OXi8006 analogues and prepare a plethora of new compounds with different functional groups. Ultimately, the objective is to discover new, more efficient tubulin-binding agents.

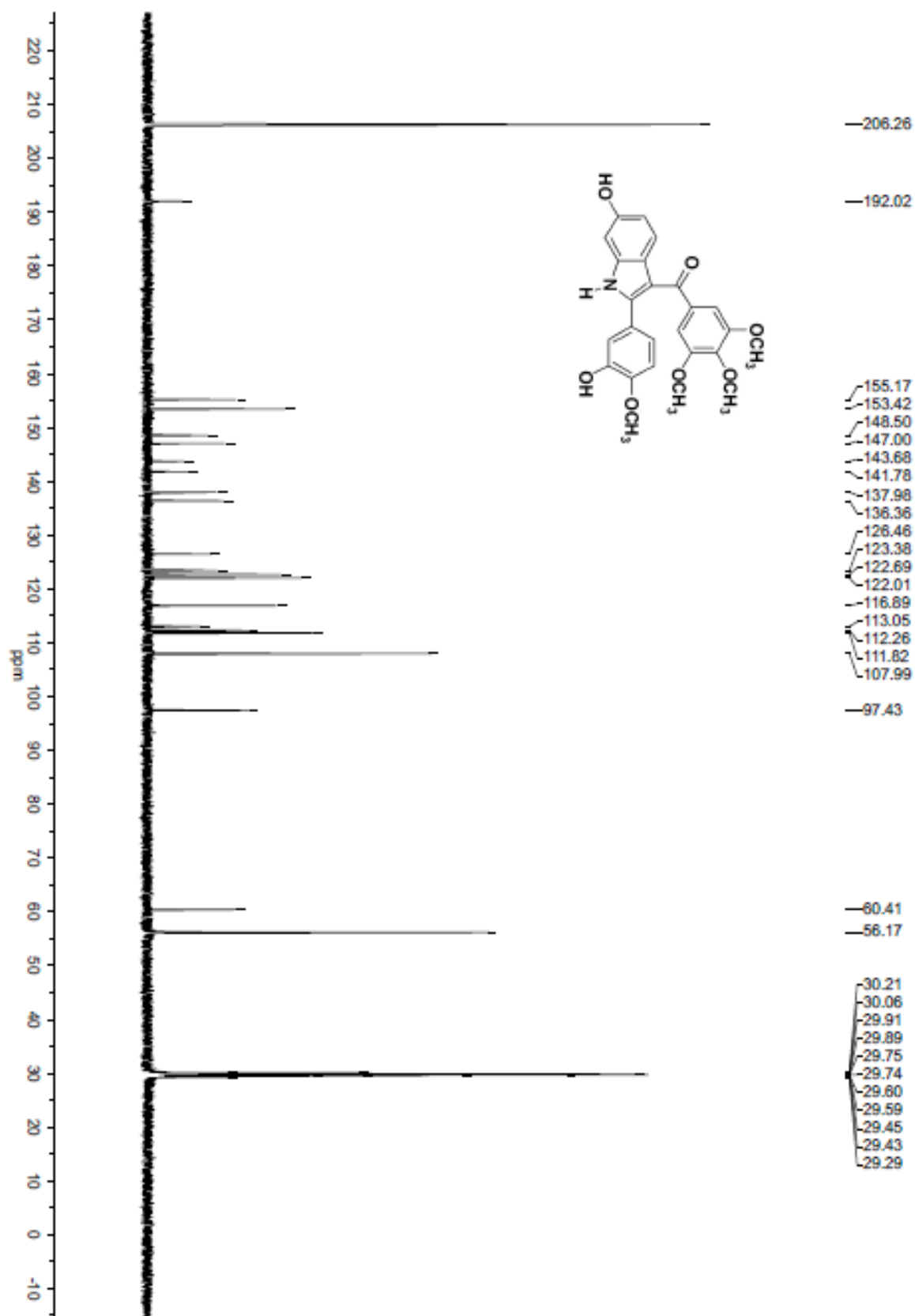
## APPENDIX

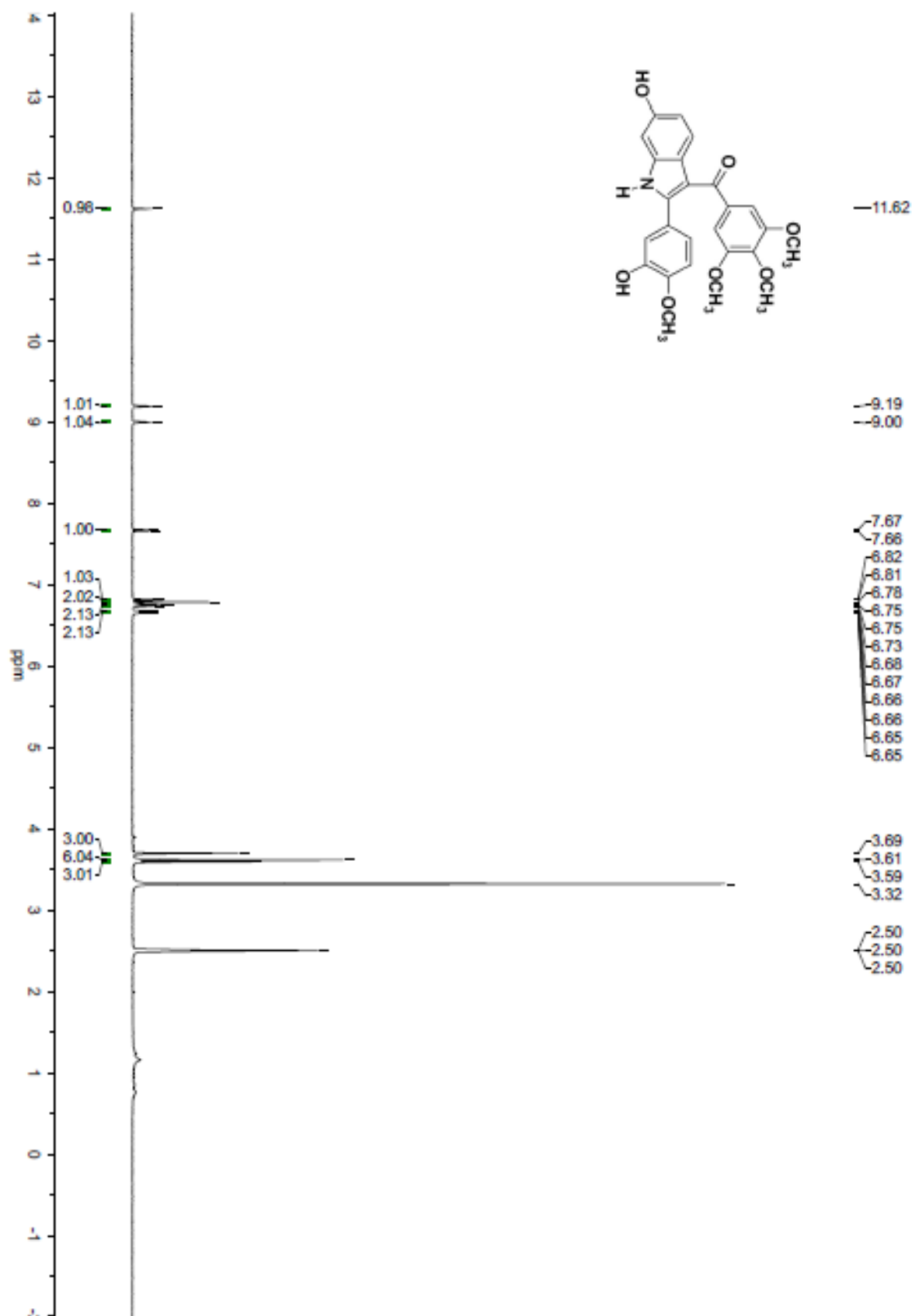
### Selected NMR spectra

$^{13}\text{C}$ NMR ( $\text{CDCl}_3$ , 125 MHz) of Compound <b>15</b>	27
$^1\text{H}$ NMR ( $\text{CDCl}_3$ , 500 MHz) of Compound <b>15</b>	28
$^{13}\text{C}$ NMR ( $(\text{CD}_3)_2\text{CO}$ , 125 MHz) of Compound <b>13</b>	29
$^1\text{H}$ NMR ( $(\text{CD}_3)_2\text{CO}$ , 500 MHz) of Compound <b>13</b>	30
$^{13}\text{C}$ NMR ( $\text{CDCl}_3$ , 125 MHz) of Compound <b>10</b>	31
$^1\text{H}$ NMR ( $\text{CDCl}_3$ , 500 MHz) of Compound <b>10</b>	32

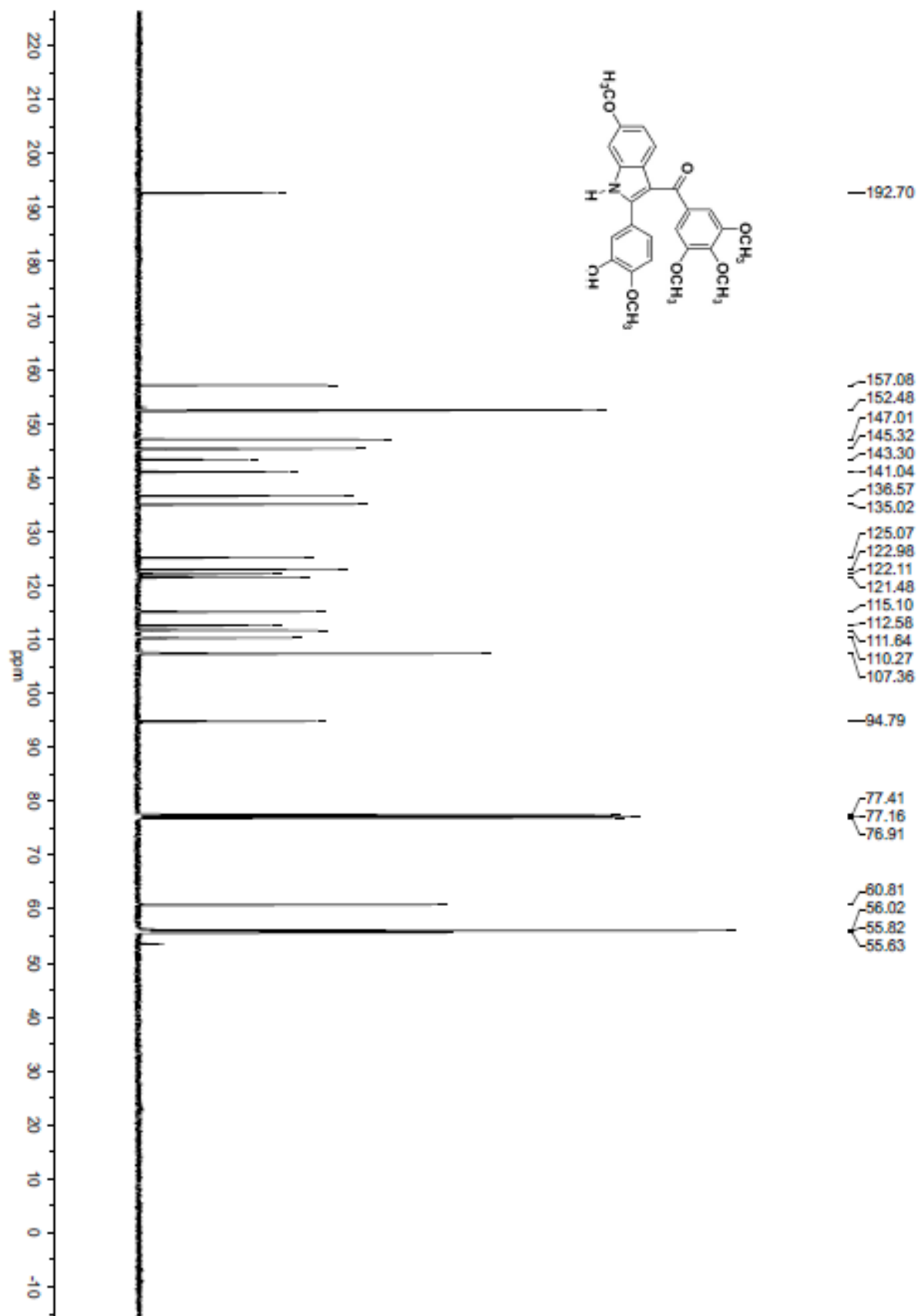


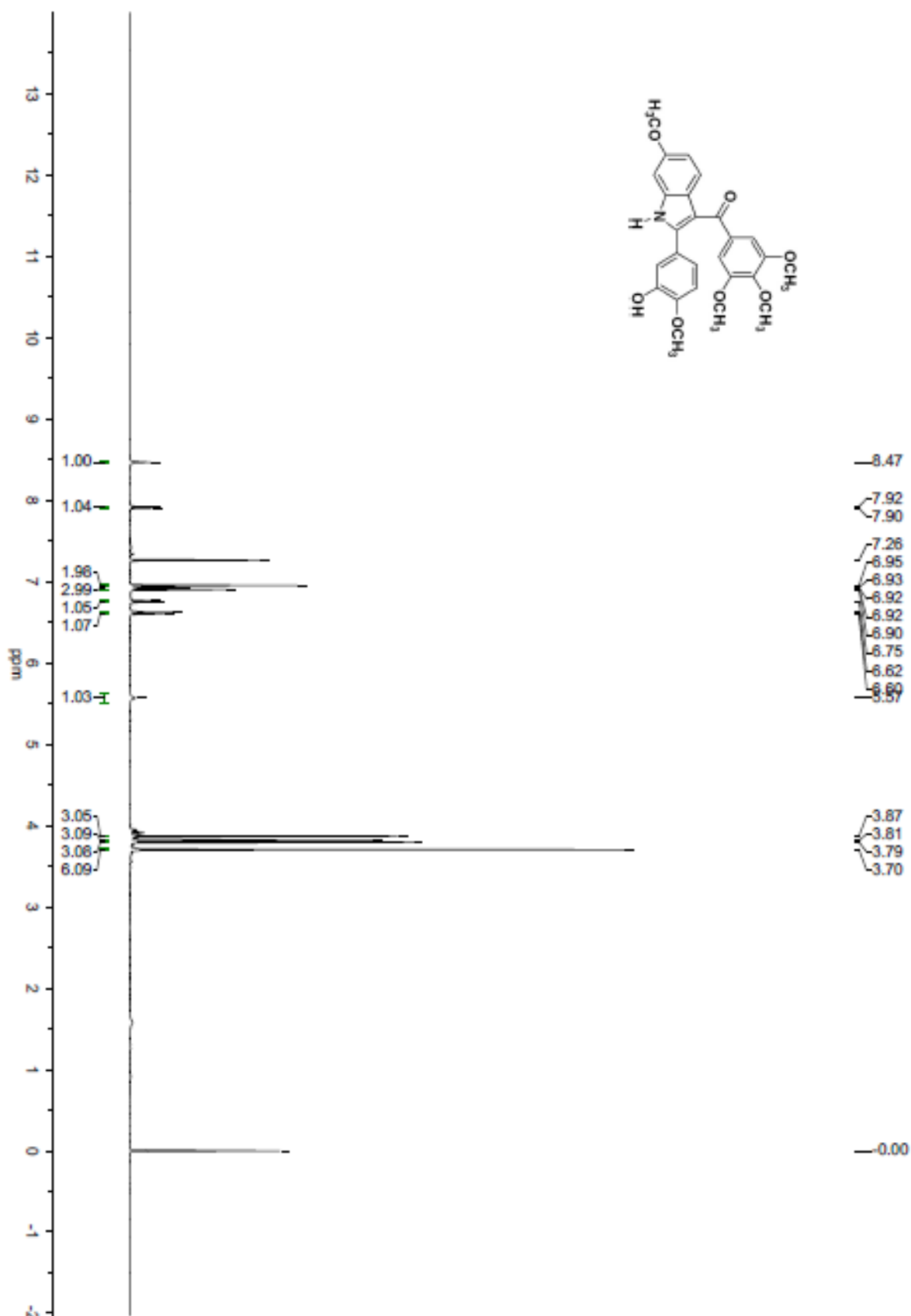












## REFERENCES

1. Siemann, D.W. *Cancer Treatment Reviews*. **2011**, 37, 63-74.
2. Kondering, M.A.; Malkusch, W.; Klapthor, B.; et al. *Br. J. Cancer*. **1999**, 80, 724-732.
3. Dewhirst, M.W.; Kimura, H.; Rehmus, S.; Braun, R.D.; Papahadjopoulos, D.; Hong, K.; Secomb, T.W. *Br J Cancer*. **1996**, 27, 247-251.
4. Vaupel, P.; Schlenger, K.; Knoop, C.; Hockel, M. *Cancer Res*. **1991**, 51, 3316-3322.
5. Denekamp, J. *Cancer Metastasis Rev*. **1990**, 9, 267-282.
6. Folkman, J.N. *Engl J Med*. **1971**, 285, 1182-1186.
7. Siemann, D.W.; Bibby, M.C.; Dark, G.G.; Dicker, A.P.; Eskens, F.A.; et al. *Clin Cancer Res*. **2005**, 11, 416-420.
8. Nakamura, K.; Taguchi, E.; Miura, T.; et al. *Cancer Res*. **2006**, 66, 9134-9142.
9. Randal, J. *J Natl Cancer Inst*. **2000**, 92, 520-522.
10. Eichhorn, M.E.; Streith, S.; Dellian, M.; *Drug. Res. Updates*. **2004**, 7, 125-138.
11. Baguley, B.C. *Lancet Oncol*. **2003**, 4, 141-148.
12. Sato, M.; Arap, W.; Pasqualini, R. *Oncology*. **2007**, 21, 1346-1352.
13. Seshadri, M.; Sperryak, J.A.; Maiery, P.G.; Cheney, R.T.; Mazarchuk, R.; Bellnier, D.A. *Neoplasia*. **2007**, 9, 128-135.
14. Pilat, M.J.; LoRusso, P.M. *J Cell. Biochem*. **2006**, 99, 1021-1039.
15. Rewcastle, G.W.; Atwell, G.J.; Baguely, B.C. *J Med Chem*. **1991**, 34, 2864-2870.
16. Thorpe, P.T. *Clin. Cancer. Res*. **2004**, 10, 415-427.
17. vaHorssen, R.; Hagen, T.L.M.; Eggermount, A.M.M. *Oncologist*. **2006**, 11, 397-408.
18. Ludford, R. *Br J Cancer*. **1948**, 2, 75-86.

19. Pettit, G.R.; Cragg, G.M.; Herald, D. *Can J. Chem.* **1982**, 60, 1374-1376.
20. Lin, C.M.; Ho, H.H.; Pettit, G.R.; Hamel, E. *Biochemistry.* **1989**, 28, 6984-6991.
21. Tozer, G.M.; Kanthouh, C.; Baguely, B.C. *Nat. Rev. Cancer.* **2005**, 5, 423-435.
22. Neri, D.; Bicknell, R. *Nat. Rev. Cancer.* **2005**, 5, 346-446.
23. Jordon, A.; Hadfield, J.A.; Lawrence, N.J.; McGown, A.T.; *Med. Res. Rev.* **1998**, 18, 259-296.
24. Downing, K.H. *Annu Rev. Cell Biol.* **2000**, 16, 89-111.
25. Sept D. *Curr. Biol.* **2007**, 17, R764-R766.
26. Jordan, M.A.; Wilson, L. *Nat. Rev. Cancer.* **2004**, 4, 253-265.
27. Rao, S.; Orr, G.A.; Chaudhary, A.G.; Kingston, D.G.I.; Horwitz, S.B. *J. Biol. Chem.* **1995**, 270, 20235-20238.
28. Lee, R.M.; Gewirtz, D.A. *Drug Dev. Res.* **2008**, 69, 352-358.
29. Sririam, M. Design, synthesis, biochemical and biological evaluation of benzocyclic and enediyne analogs of combretastatins as potential tubulin binding ligands in the treatment of cancer. Ph.D. Dissertation, Baylor University, Waco, Texas, December 2007.
30. Pettit, G.R.; Cragg, G.M.; Singh, S. B. *J. Nat. Prod.* **1987**, 50, 386-389.
31. El-Zayat, A. A. E.; Degen, D.; D., Sonya; C., Gary M.; Pettit, G. R.; Von Hoff, D. *Anti-Cancer Drugs.* **1993**, 4, 1, 19-25.
32. Pettit, G.R.; Lippert (III), J.W.; Herald, D.L; Hamel, E; Pettit, R.K. *J. Nat. Prod.* **2000**, 63, 969-974.
33. Shi, Q; Chen, K; Morris-Natschke, S, L; Lee, K. *Curr. Pharm. Design*, **1998**, 4, 219-24833.
34. Gaukroger, K; Hadfield, J. A; Lawrence, N. J; Nolan, S; McGown, A. T. *Org. Biomol. Chem.* **2003**, 1, 3033-3037.
35. Pinney, K. G; Arthasery, P; Shirali, A; Edvardsen, K; Chaplin, D. J. U.S. Patent 2005245489, **2005**
36. Cragg, D.J.; Kingston, G.M.; Newman, D.G.I. *Anti-Cancer Agents from Natural Products*. Second Ed. 2011, 27-65.

37. Bischler, A.; Brion, H. *Chem. Ber.* **1892**, 25, 2860.
38. Bischler, A.; Firemann, P. *Chem. Ber.* **1893**, 26, 1336.
39. Mohlau, R. *Chem. Ber.* **1881**, 14, 173.
40. Mason, R.P.; Dawen, Z.; Liu, L.; Trawick, M.L.; Pinney, K.G. *Integr. Biol.* **2011**, 3, 375-387.

# Baylor University – Honors College – Thesis Copyright and Availability Form

Scan this **completed and signed** form as a PDF for submission to BEARdocs along with your thesis.

Date: April 27, 2012

Student's Full Name (First, Middle, and Last Name): Priscilla Sotn Hoz

Date of Birth (mm-dd-yyyy): 10/26/1989

Permanent Email Address: 1

Date of Graduation (mm-yyyy): May 2012

Major(s): Biochemistry, B.S.

Thesis Title: Structural Modifications of OX18006 Leading to New Indole-Based Anti-Cancer Agents

## BAYLOR UNIVERSITY COPYRIGHT AGREEMENT

I certify that the version of the thesis that I submitted is the same as that approved by the thesis chairperson, the thesis committee, and the Honors College.

I hereby grant to Baylor University or its agents the non-exclusive license to archive and make accessible, under the conditions specified below, my thesis, dissertation, or record of study in whole or in part in all forms of media, now or hereafter known.

**FERPA.** To the extent this thesis, dissertation, or record of study is an educational record as defined in the Family Educational Rights and Privacy Act (FERPA) (20 USC 1232g), I consent to disclosure of it to anyone who requests a copy.

I retain all other ownership rights to the copyright of the thesis, dissertation or record of study.

I also retain the right to use in future works (such as articles or books) all or part of this thesis, dissertation, or record of study.

## AVAILABILITY OPTIONS (check one)

☐ 1. Release the work immediately for **worldwide access on the Internet**.  
(Recommended for most theses.)

☒ 2. Secure the work for **two years**, then release the work for **worldwide access on the Internet**.  
(One-year extension, **upon request**, if needed.)

## Thesis Chairperson's Signature

I have discussed the availability choices with this student, and I am aware of the choice this student has made.

Chair/Co-chair's Signature: [Signature]

## STUDENT AVAILABILITY & COPYRIGHT AGREEMENT

I have read and fully agree to the Baylor University copyright agreement regarding my thesis. I agree to the thesis availability option I selected above. I understand that the availability option is my choice and that there may be publishing consequences to my selection.

Student's Signature: [Signature]

## Baylor University's Policy

Your thesis will be made available shortly after graduation **worldwide on the Internet** via BEARdocs (<http://beardocs.baylor.edu>), unless you choose to delay release.

**Questions about availability options?** If you still have questions or concerns about availability options, please e-mail us at [libraryquestions@baylor.edu](mailto:libraryquestions@baylor.edu).